CLE Peptides Control *Medicago truncatula* Nodulation Locally and Systemically[1][C][W][OA]

Virginie Mortier, Griet Den Herder, Ryan Whitford, Willem Van de Velde, Stephane Rombauts, Katrien D'haeseleer, Marcelle Holsters*, and Sofie Goormachtig

Department of Plant Systems Biology, VIB, B–9052 Ghent, Belgium; and Department of Plant Biotechnology and Genetics, Ghent University, B–9052 Ghent, Belgium

The CLAVATA3/embryo-surrounding region (CLE) peptides control the fine balance between proliferation and differentiation in plant development. We studied the role of CLE peptides during indeterminate nodule development and identified 25 MtCLE peptide genes in the *Medicago truncatula* genome, of which two genes, *MtCLE12* and *MtCLE13*, had nodulation-related expression patterns that were linked to proliferation and differentiation. *MtCLE13* expression was up-regulated early in nodule development. A high-to-low expression gradient radiated from the inner toward the outer cortical cell layers in a region defining the incipient nodule. At later stages, *MtCLE12* and *MtCLE13* were expressed in differentiating nodules and in the apical part of mature, elongated nodules. Functional analysis revealed a putative role for *MtCLE12* and *MtCLE13* in autoregulation of nodulation, a mechanism that controls the number of nodules and involves systemic signals mediated by a leucine-rich repeat receptor-like kinase, SUNN, which is active in the shoot. When *MtCLE12* and *MtCLE13* were ectopically expressed in transgenic roots, nodulation was abolished at the level of the nodulation factor signal transduction, and this inhibition involved long-distance signaling. In addition, composite plants with roots ectopically expressing *MtCLE12* or *MtCLE13* had elongated petioles. This systemic effect was not observed in transgenic roots ectopically expressing *MtCLE12* and *MtCLE13* in a *sunn-1* mutant background, although nodulation was still strongly reduced. These results suggest multiple roles for CLE signaling in nodulation.

In the symbiotic interaction between legume plants and rhizobia, root nodules develop within which the bacteria fix atmospheric nitrogen. Nodule development requires the spatiotemporal orchestration of developmental programs for infection and organ formation (Jones et al., 2007). In *Medicago truncatula*, the microsymbiont *Sinorhizobium meliloti* enters via curled root hairs and transcellular infection threads. While infection is taking place, inner cortical and pericycle cells divide and form the nodule primordium. The infection threads penetrate primordium cells, and bacteria are released into the plant cytoplasm within membrane-enclosed symbiosomes. Inside the symbiosomes, the bacteria differentiate into bacteroids and start the nitrogen fixation process (Jones et al., 2007). Meanwhile, an apical meristem develops and provides new cells for bacterial internalization. The nodules are of the indeterminate type and have a cylindrical shape.

The perception of bacterial signaling molecules, the nodulation factors (NFs), by specific LysM-type receptor-like kinases (RLKs) in the epidermis of the host plant elicits various responses to allow root hair invasion and cell division (Madsen et al., 2003; Radutoiu et al., 2003, 2007; Jones et al., 2007; Oldroyd and Downie, 2008). While the inner cortical cells divide, outer cortical cells arrest in the G2 phase of the cell cycle, resulting in cytoplasmic bridges, the preinfection threads, through which the infection threads grow (Yang et al., 1994; van Spronsen et al., 2001).

Opposite preexisting and NF-induced signal gradients have been proposed to rule the cortical cell responses (Smit et al., 1995; Heidstra et al., 1997; van Spronsen et al., 2001). Uridine and ethylene are diffusive signals originating from the vasculature that have been identified as positive and negative regulators, respectively. In white clover (*Trifolium repens*), the auxin flow within the root vasculature was transiently inhibited at the site of infection, leading to auxin accumulation in the cortical region where the nodule primordia form (Mathesius et al., 1998). A reduction in auxin flow has been confirmed by radioactive auxin tracer experiments for *M. truncatula* and vetch (*Vicia faba*) but not *Lotus japonicus* (Boot et al., 1999; Pacios-Bras et al., 2003; van Noorden et al., 2006; Wasson et al.,

[1] This work was supported by the Ministerie van de Vlaamse Gemeenschap (grant no. CLO/IWT/020714), by the Research Foundation-Flanders (grant nos. G.0350.04N and 3G006607 and predoctoral fellowship to K.D.), and by the Agency for Innovation by Science and Technology in Flanders (predoctoral fellowship to G.D.H.).

* Corresponding author; e-mail marcelle.holsters@psb.vib-ugent.be.

The author responsible for distribution of materials integral to the findings presented in this article in accordance with the policy described in the Instructions for Authors (www.plantphysiol.org) is: Marcelle Holsters (marcelle.holsters@psb.vib-ugent.be).

[C] Some figures in this article are displayed in color online but in black and white in the print edition.

[W] The online version of this article contains Web-only data.

[OA] Open Access articles can be viewed online without a subscription.

www.plantphysiol.org/cgi/doi/10.1104/pp.110.153718

2006). Cytokinins are essential for nodule development because *L. japonicus* knockout mutants for the cytokinin receptor gene, *LHK1*, or *M. truncatula* transgenic plants with suppressed expression of the ortholog, *CRE1*, were defective in nodule primordia formation (Gonzalez-Rizzo et al., 2006; Murray et al., 2007). Additionally, a *L. japonicus* gain-of-function mutant for the LHK1 receptor provoked spontaneous nodules, indicating that cytokinin signaling is both necessary and sufficient for nodule formation (Tirichine et al., 2007).

Several components that link NF signaling to the initiation of cortical cell division have been identified. In *M. truncatula*, NF perception by LysM-type RLKs at the epidermis activates a signaling cascade that is mediated by the leucine-rich repeat (LRR)-RLK, Doesn't Make Infections2 (DMI2), and the nuclear potassium channel, DMI1. This signaling cascade triggers Ca^{2+} spiking in and around the nucleus. Decoding of this Ca^{2+} signature by a Ca^{2+} calmodulin-binding protein (DMI3) results in the activation of the transcription factors Nodulation Signaling Pathway1 (NSP1), NSP2, Ethylene-Responsive Binding Domain Factor Required for Nodulation1 (ERN1), and Nodule Inception (NIN; Schauser et al., 1999; Catoira et al., 2000; Borisov et al., 2003; Oldroyd and Long, 2003; Gleason et al., 2006; Andriankaja et al., 2007; Marsh et al., 2007; Middleton et al., 2007; Oldroyd and Downie, 2008). NSP2, ERN1, and NIN also play a role downstream of the cytokinin signaling to trigger cortical cell division (Tirichine et al., 2007; Frugier et al., 2008).

Nodule formation and functioning are energy-consuming processes, and legumes have evolved several strategies to control the number of nodules. One such strategy, autoregulation of nodulation (AON; Kosslak and Bohlool, 1984), is activated when the first nodules develop and involves systemic signals and shoot-controlled factors (Magori and Kawaguchi, 2009). Insight into this mechanism has been obtained by the identification of supernodulation mutants of soybean (*Glycine max*; *nts-1*), *M. truncatula* (*sunn*), *L. japonicus* (*har1*), and pea (*Pisum sativum*; *sym29*), each of which is deficient in an LRR-RLK that is required in shoots for AON (Krusell et al., 2002; Nishimura et al., 2002; Searle et al., 2003; Schnabel et al., 2005). Auxin might be implicated in this process because *sunn-1* mutants display a higher level of long-distance shoot-to-root auxin transport than wild-type plants. Importantly, in contrast to the wild type, this transport is not reduced upon nodulation (van Noorden et al., 2006).

The LRR-RLKs responsible for AON belong to the evolutionary clade of group XI RLKs (Shiu and Bleecker, 2001) that includes the Arabidopsis (*Arabidopsis thaliana*) receptors CLAVATA1 (CLV1), PXY-like1 (PXL1) and PXL2, BARELY ANY MERISTEM1 (BAM1) to BAM3, and the putative tracheary element differentiation inhibitory factor (TDIF) receptor (TDR; Clark et al., 1997; DeYoung et al., 2006; Fisher and Turner, 2007; Hirakawa et al., 2008; Ogawa et al., 2008). These LRR-RLKs bind or putatively recognize CLV3/embryo-surrounding region (CLE) peptides (Hirakawa et al., 2008; Ogawa et al., 2008) that are a group of small (12–13 amino acids) secreted peptides derived from the C-terminal region of preproproteins (Mitchum et al., 2008; Oelkers et al., 2008). The Arabidopsis genome contains 32 gene family members, of which the best studied is CLV3, the peptide ligand for a CLV1-containing cell surface receptor complex. Recognition of the CLV3 peptide is important for stem cell homeostasis within the shoot apical meristem (SAM; Ogawa et al., 2008), whereas TDIF, a phloem-secreted CLE peptide, binds in vitro the PXY/TDR receptor expressed in the procambial cells and inhibits vascular differentiation (Hirakawa et al., 2008).

CLE peptides with related sequences exhibit redundancy, as proven by similarity in gain-of-function phenotypes (Strabala et al., 2006; Jun et al., 2008). At least two groups of CLE peptides can be distinguished. Group I peptides, exemplified by CLV3, result in premature root and shoot meristem growth arrest when exogenously applied or ectopically expressed, indicating that they are promoters of cellular differentiation. Members of group II, exemplified by TDIF, prevent cellular differentiation, as evidenced by the suppression of procambium-to-xylem transdifferentiation in zinnia (*Zinnia elegans*) cell cultures, and control the rate and orientation of vascular cell division (Ito et al., 2006; Etchells and Turner, 2010). Although these studies would suggest two groups with opposing functions, synergistic actions between these groups of peptides have been demonstrated (Whitford et al., 2008). In Arabidopsis, the proliferation of vascular precursor cells induced by the group II CLE41 peptides is enhanced by the addition of CLE6 peptides that otherwise have an inhibiting effect on root growth when applied at high concentrations and thus belong to group I. Moreover, genetic studies with *clv3*, *clv1*, and *bam* mutants reveal complex spatiotemporally controlled interactions between putative ligand/receptor complexes (DeYoung and Clark, 2008).

Cellular dedifferentiation and differentiation processes act at sequential stages of nodule development. At nodule initiation, pericycle and cortical cells dedifferentiate and divide (van Brussel et al., 1992; Timmers et al., 1999; van Spronsen et al., 2001). When sufficient cells encompassing the nodule primordia have formed, division ceases and the cells differentiate and become infected with rhizobia. Meanwhile, for indeterminate nodules, an apical meristem is established that supplies a constant pool of cells for bacterial infection. Hence, CLE peptides might not only be involved in AON but also regulate the (de)differentiation processes that control nodule development.

We analyzed the role of CLE peptides in *M. truncatula* nodulation. By specialized BLAST searches, nine peptide genes were identified in the Mt2.0 release in addition to the 16 previously discovered (Cock and McCormick, 2001; Oelkers et al., 2008). Two genes, designated *MtCLE12* and *MtCLE13*, were differen-

tially expressed during nodule development. The expression patterns hint at roles during (de)differentiation throughout nodule development. Moreover, when *MtCLE12* and *MtCLE13* were ectopically overexpressed, an inhibition of nodulation by long-distance signaling was observed. Furthermore, transgenic plants bearing roots expressing *35S:MtCLE12* or *35S:MtCLE13* had elongated petioles, a systemic effect not observed in *sunn-1* mutants, although nodulation was still strongly hampered.

RESULTS

Search for Up-Regulated *MtCLE* Genes during Nodulation

Besides the 16 putative *M. truncatula CLE* genes described (Cock and McCormick, 2001; Oelkers et al., 2008), we searched for additional *MtCLE* genes in the EST databases (www.tigr.org/tdb/tgi/) and in the *M. truncatula* genomic data (Mt2.0) with a PAM30 tBLASTn homology-based algorithm to identify peptide sequences corresponding to the conserved CLE motif (Supplemental Table S1). Twenty-five *MtCLE* candidates were identified and designated *MtCLE1* to *MtCLE25* (Supplemental Fig. S1). The corresponding CLE preproproteins varied in length between 45 and 221 amino acids and had a high level of sequence divergence outside the CLE motif (Supplemental Fig. S1). Except for MtCLE3, all proteins contained an N-terminal signal peptide as predicted by HMM SignalP and neural networks (Bendtsen et al., 2004). Two MtCLE peptide candidates contained multiple CLE domains, namely MtCLE14 and MtCLE22 that had seven and three tandemly arranged CLE domains, respectively.

To determine tissue- or organ-specific expression, quantitative reverse transcription (qRT)-PCR was carried out for each *MtCLE* candidate on cDNAs derived from root elongation zones, nodulated roots (1 month post inoculation), root tips, stems, SAMs, cotyledons, first leaves, and mature leaves. cDNA of root elongation zones was used as the reference tissue. Transcripts were detected for 15 of the 25 identified *MtCLE* genes, of which 10 required 30 or more PCR cycles, indicating low transcript levels or cell-specific expression. *MtCLE2*, *MtCLE4*, *MtCLE5*, *MtCLE11*, *MtCLE15*, and *MtCLE24* were mainly expressed in root tissues, *MtCLE1*, *MtCLE16*, and *MtCLE23* were expressed predominantly in shoot tissues, and *MtCLE6*, *MtCLE12*, and *MtCLE17* were expressed in several plant tissues (Fig. 1A). For *MtCLE3* and *MtCLE13*, expression was restricted to stems and cotyledons and to nodulated roots, respectively, while for *MtCLE20*, transcripts

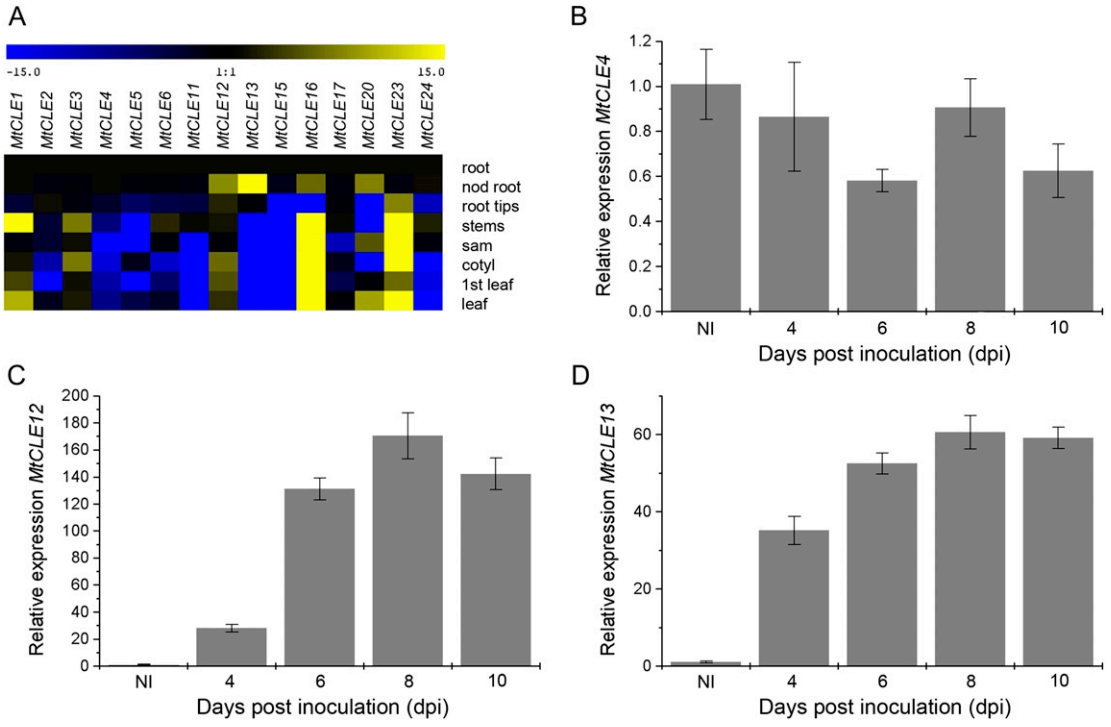

Figure 1. Expression analysis of *MtCLE* genes. A, Heat map of *MtCLE* expression in different tissues as measured by qRT-PCR. Samples are cDNA from root elongation zones (root), nodulated roots 1 month post inoculation (nod root), root tips, stems, SAMs (sam), cotyledons (cotyl), first leaves (1st leaf), and mature leaves (leaf). B to D, Expression analysis of *MtCLE4*, *MtCLE12*, and *MtCLE13*, respectively, by qRT-PCR on cDNA samples of zone I root tissues of uninoculated plants (NI) and at 4, 6, 8, and 10 dpi.

were detected in nodulated roots, leaves, and SAMs. Four *MtCLE* genes (*MtCLE12*, *MtCLE13*, *MtCLE16*, and *MtCLE20*) were more abundantly transcribed in nodulated than in control roots (Fig. 1A). Biological repeats, however, only consistently confirmed the differential expression of *MtCLE12* and *MtCLE13*.

To study the temporal expression during nodule development, the relative transcript level of each *MtCLE* gene was analyzed at 4, 6, 8, and 10 d post inoculation (dpi). The elongation zone of uninoculated roots, the nodule initiation site, was used as the reference tissue. *MtCLE12* expression was low at 4 dpi (Fig. 1C) but increased until 6 dpi and remained high until 10 dpi. *MtCLE13* transcript increased until 10 dpi (Fig. 1D). As we were interested in the function of CLE peptides during nodulation, *MtCLE12* and *MtCLE13* were selected for further analysis and compared with *MtCLE4*, given its root-specific expression (Fig. 1, A and B).

As shown in Supplemental Table S2, the CLE peptide sequences of MtCLE12 and MtCLE13 differ by four amino acids. We analyzed the homology of MtCLE12, MtCLE13, and MtCLE4 to Arabidopsis CLE peptides. MtCLE12 and MtCLE13 were most similar to AtCLE1 to AtCLE7 and MtCLE4 to AtCLE9/10. Upon *L. japonicus* nodulation, three *CLE* genes were described to be up-regulated (Okamoto et al., 2009). Peptides derived from MtCLE12 and MtCLE13 only differed by three and one amino acids (an A/G change at position 4) from the identical LjCLE-RS1 and LjCLE-RS2, respectively.

Effects of Exogenous Application of MtCLE4, MtCLE12, and MtCLE13 Peptides on Root Growth and Nodulation

To check the effect on root growth, we supplied 10 μM of chemically synthesized peptides corresponding to the CLE domain of these three proteins (MtCLE4p, MtCLE12p, and MtCLE13p; see "Materials and Methods") exogenously to the primary roots of 2-d-old seedlings. Root length was measured after 8 d of growth. As controls, seedlings were grown on medium either supplemented or not (no peptide) with a synthetic 16-amino acid peptide corresponding to the C terminus of the Arabidopsis AGAMOUS protein. Primary root length for 16 plants per treatment was measured (Fig. 2). After addition of MtCLE12p or MtCLE13p, an average root length of 91.0 $\pm$ 13.2 and 103.4 $\pm$ 5.8 mm was observed, respectively, which did not differ significantly from the average root length with (101.9 $\pm$ 8.0 mm) and without (97.0 $\pm$ 6.2 mm) addition of the control peptide. For the seedlings treated with MtCLE4p, the average primary root length was 73.8 $\pm$ 8.0 mm, which is 24% shorter than the controls. The difference in number of lateral roots per primary root was not statistically significant. Exogenous peptide application (10–50 μM) had no effect on the nodule number.

MtCLE12 and *MtCLE13* Expression Pattern in Roots and Developing Nodules

Spatial expression patterns of *MtCLE12* and *MtCLE13* in roots and developing nodules was investigated by *promoter*:*GUS* analysis and in situ hybridizations. A 2-kb region upstream of *MtCLE12* and *MtCLE13* was isolated based on the available genomic data (http://www.ncbi.nlm.nih.gov/) and cloned 5′ to the *uidA* gene. Transcriptional activation of the *uidA* gene was visualized by GUS staining.

No GUS staining was observed in uninoculated transgenic roots. At 3 dpi, *MtCLE13* expression was detected in cell clusters along root zones susceptible to rhizobial infection (Fig. 3A). At that time point, some incipient nodule primordia were present, but not all were at the same stage on a single root. As a result, between the most developed primordia and the root tip, many more incipient nodulation events occurred, and the closer to the root tip, the less developed the primordia. Inoculations with *Sm2011-mRFP*, carrying the monomeric red fluorescent protein (mRFP), revealed that *pMtCLE13*:*GUS* was expressed only in regions of bacterial infection. Careful comparison of the infection events with the GUS staining patterns indicated that the *pMtCLE13*:*GUS* expression could be followed down to nodulation events in which only curled colonized root hairs were visible. Sections of these infected regions revealed that these clusters corresponded to early nodulation stages without or with only a few cell divisions. Closest to the root tip, the *pMtCLE13*:*GUS* expression was mainly localized in inner cortical cells (Fig. 3, B and C), scattered in outer cortical cells (Fig. 3B), and absent in the pericycle and vascular tissues (Fig. 3, B and C). At positions where cell division was more pronounced in the inner cortex, the GUS staining pattern was more intense in the dividing cells (Fig. 3, C–E). A decreasing gradient of *pMtCLE13*:*GUS* expression radiated from the inner to the outer cortical cells and pericycle (Fig. 3, C–E).

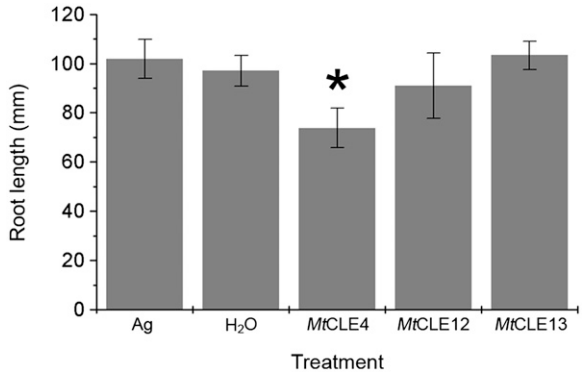

Figure 2. Effect of in vitro application of MtCLE4, MtCLE12, and MtCLE13 peptides on the root length of *M. truncatula*. The plants were grown for 6 d on plates containing 10 μM peptides (n = 39 for each treatment). As a control, plants were not treated (H_2O) or were treated with the AGAMOUS (Ag) peptide. Data and error bars represent means $\pm$ SD. The asterisk marks a statistically different group.

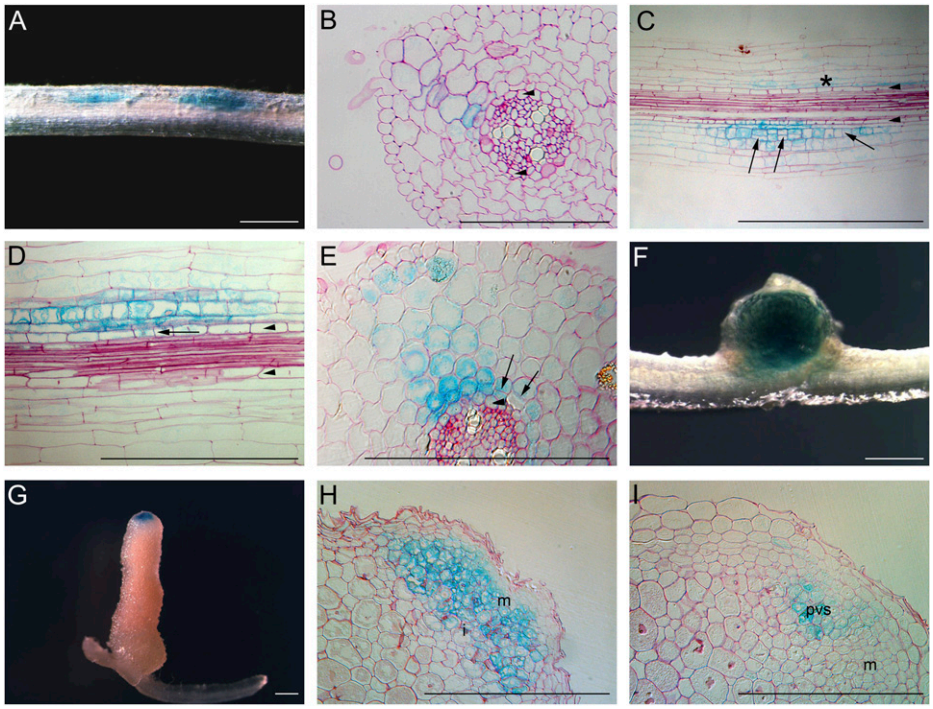

Figure 3. *MtCLE13* promoter activity during nodulation. A, Transgenic *pMtCLE13*:*GUS* root segment of the susceptible root zone I at 3 dpi. GUS staining was observed in patches along the root. B, Transverse section through a root segment at an initial stage of nodule formation when still no cell divisions occur. Blue staining is the highest in the inner cortical cells. Arrowheads indicate pericycle. C and D, Longitudinal sections through the root segment shown in A. In the incipient nodulation event (indicated by an asterisk in C), staining is seen in inner cortical cells but not in the pericycle cells. In slightly more developed nodule primordia, where cell divisions are visible in cortex and pericycle (examples marked by arrows in C and D), GUS staining is the strongest in the dividing cells of the cortex but also in the pericycle. E, Transverse section through a young developing nodule primordium at a stage similar to that in D. Cell division is clearly visible in the cortex (arrows). The pericycle cell file is indicated by arrowheads (in C–E). *pMtCLE13*:*GUS* is expressed in the cortex and at a low level in the pericycle, with the highest expression in the dividing inner cortical cells. F, A round, young nodule with GUS staining throughout the nodule tissue. G, GUS staining of a mature, elongated nodule. H, Longitudinal section through an elongated nodule. GUS staining is seen in the meristematic tissue and early infection zone. I, Longitudinal section through an elongated nodule, in which the expression is the highest in cells that presumably correspond to the provascular strands. i, Infection zone; m, meristem; pvs, provascular strands. Bars = 1 mm (A, B, D, F, and G) and 0.5 mm (C, E, H, and I).

Expression was highest in the dividing cortical cells, but dividing pericycle cells displayed GUS staining as well. In round, young nodules, GUS staining was seen throughout the central tissue (Fig. 3F). In elongated nodules, it was restricted to the apical region, corresponding to the meristematic and early infection zones (Fig. 3, G and H). Although mostly all the meristematic cells were blue, in some nodules the expression was the highest in cells that corresponded to the provascular system (Fig. 3I). In situ hybridizations revealed a similar expression pattern, with low transcript levels in the meristem and cells of the early infection zone (Supplemental Fig. S2). For some nodules, *MtCLE13* transcripts were more clearly detectable in cells of the provascular strands (Supplemental Fig. S2, C and D).

For *pMtCLE12*:*GUS*, no expression was detectable at the earliest stages of nodule development (Fig. 4A) but appeared in young round nodules (Fig. 4B). Later in nodule development, *pMtCLE12*:*GUS* was restricted to the apical zone of elongated nodules, similar to *pMtCLE13*:*GUS* (Fig. 4, C and D).

MtCLE12 and *MtCLE13* Expression in Nodulation Mutants

To investigate whether NF signaling is required for the induction of *MtCLE12* and *MtCLE13* expression, we analyzed the transcript levels by qRT-PCR before and after inoculation of *nin*, the *ERN1* mutant *branching infection threads1-1* (*bit1-1*), *nsp1*, *nsp2*, *dmi1*, *dmi2*, and *dmi3* mutants (Fig. 5). The mutant lines did not develop nodules, except for *bit1-1*, which formed arrested primordia and infection foci (Andriankaja et al., 2007; Middleton et al., 2007). For *MtCLE12*, gene expression was induced upon inoculation in wild-type *M. truncatula* roots (Fig. 5A) but not in roots of the nodulation mutants, and likewise for *MtCLE13* transcripts, except in *bit1-1*, albeit less abundantly than

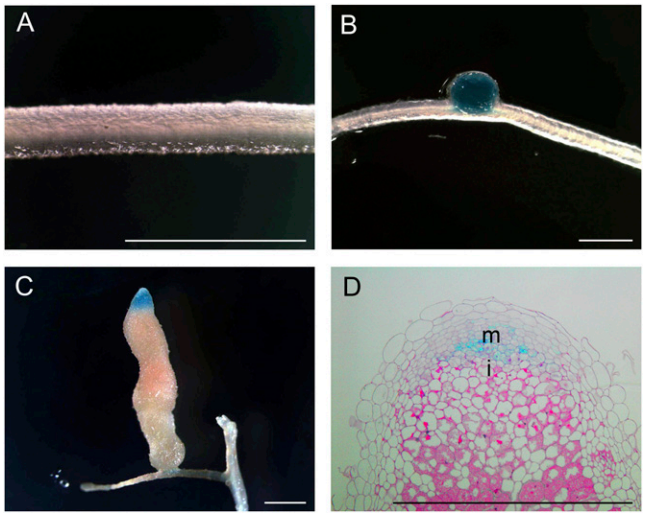

Figure 4. *MtCLE12* promoter activity during nodulation. A, *pMtCLE12*:*GUS* transgenic root segment of the susceptible root zone I at 3 dpi. No GUS staining is observed. B, GUS analysis of a young round nodule. *MtCLE12* is expressed throughout. C, GUS analysis of a mature elongated nodule. Blue staining is observed in the apical part. D, Longitudinal section through C. i, Infection zone; m, meristem. Bars = 2 mm.

upon wild-type inoculation. The expression levels of *MtCLE4* in the different mutants before and after inoculation were the same as those in the inoculated wild-type roots.

As a confirmation of the qRT-PCR analysis, *pMtCLE13*:*GUS* transgenic roots were generated in each of the mutant backgrounds and analyzed at 5 dpi. Because nodulation events are not synchronized in *M. truncatula*, consecutive early nodulation stages, ranging from stages with only a few cell divisions to young nodule primordia, could be observed along the root at 5 dpi. GUS staining revealed the typical *MtCLE13* cluster pattern in the wild-type roots. The *bit1-1* mutant was the only mutant in which blue-stained cortical regions were seen, corresponding to infection (Fig. 5C). The other mutants displayed no GUS staining. These data are in agreement with the qRT-PCR data and reveal that *MtCLE13* expression is linked with the NF-induced cortical cell activation.

Induction of *MtCLE12* and *MtCLE13* Transcription by Auxin and Cytokinin

A correct auxin/cytokinin balance is a prerequisite for nodule formation (Oldroyd and Downie, 2008; Ding and Oldroyd, 2009). To determine whether auxins and/or cytokinins affect *MtCLE12* and *MtCLE13* expression, 10^{-6} M indole-3-acetic acid (IAA) or 10^{-7} M 6-benzylaminopurine (BAP) was supplemented to the growth medium of 5-d-old seedlings. The roots of 18 seedlings were harvested under each condition after 0, 3, 6, 12, 24, and 96 h. Roots from plates without hormone addition were used as a negative control.

No significant differences in *MtCLE12* expression were detected in treated versus control roots. Auxin addition had no influence on the expression of *MtCLE13* (Fig. 6), but in roots treated with 10^{-7} M BAP, *MtCLE13* transcripts were up-regulated after a 3-h treatment and levels further increased with extended treatment times (up to 24 h; Fig. 6).

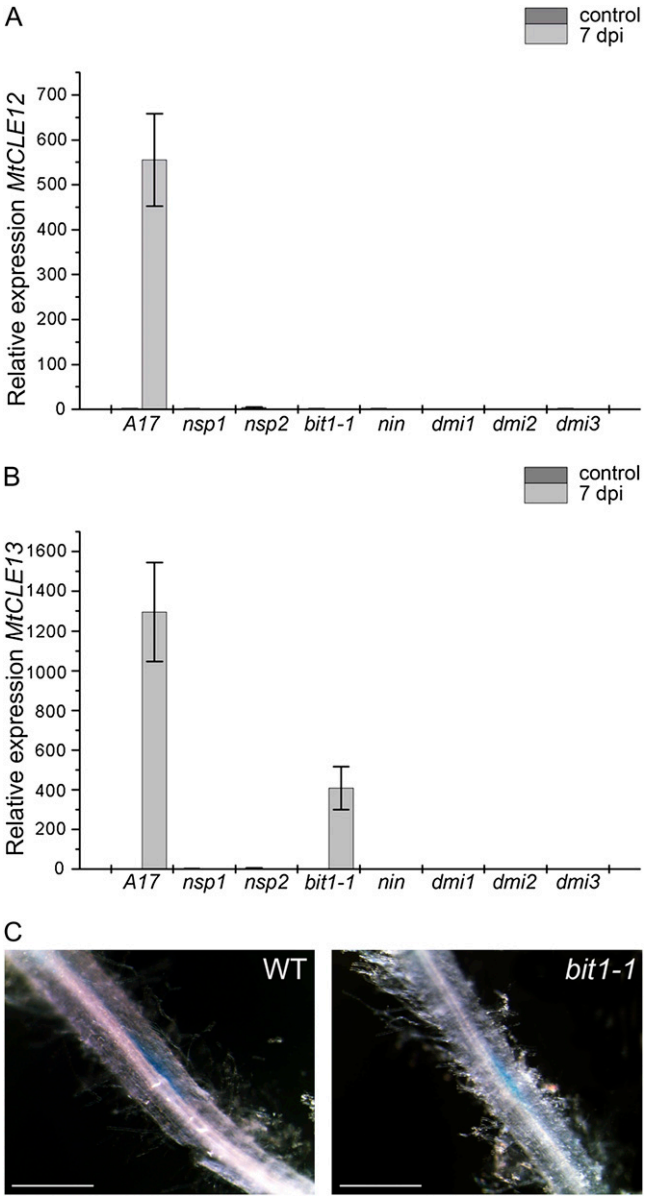

Figure 5. *MtCLE12* and *MtCLE13* expression in nodulation mutants. A and B, Expression analysis of *MtCLE12* and *MtCLE13* by qRT-PCR on cDNA samples of zone I root tissues of wild-type plants (A17) and *nsp1*, *nsp2*, *bit1-1*, *nin*, *dmi1*, *dmi2*, and *dmi3* mutants before inoculation (control) and at 7 dpi. C, *pMtCLE13*:*GUS* activity at 5 dpi in the roots of a wild-type plant (WT) and in a *bit1-1* mutant. Bars = 1 mm. [See online article for color version of this figure.]

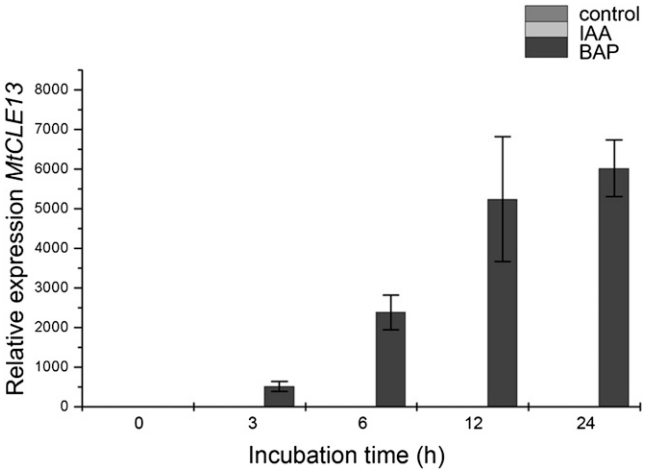

Figure 6. Influence of auxin and cytokinin on *MtCLE13* expression. qRT-PCR analysis of *MtCLE13* expression in cDNA samples of roots grown in the presence of 10^{-6} M auxin (IAA) or 10^{-7} M cytokinin (BAP). Growth medium without hormones was used for the control plants. Samples of 5-d-old plants were taken at 0, 3, 6, 12, and 24 h after hormone addition.

Effect of Ectopic Expression of *35S:MtCLE12* and *35S:MtCLE13* on Nodulation

To analyze the functions of *MtCLE4*, *MtCLE12*, and *MtCLE13*, composite plants were made that carried transgenic roots ectopically overexpressing one of the three *MtCLE* genes. Nodulation of these transgenic roots was assessed at 21 dpi. Nodulation of control transgenic roots (*35S:GUS*) resulted on average in 11 ± 4 nodules per root (Fig. 7A). On the *35S:MtCLE4* transgenic roots, an average of 10 ± 4 nodules were counted. No nodules were detected on *35S:MtCLE12* and *35S:MtCLE13* transgenic roots (Fig. 7A). qRT-PCR analysis confirmed the ectopic overexpression of the respective constructs.

To determine at what stage these two CLE peptides affect nodulation, we investigated whether ectopic overexpression of *MtCLE12* and *MtCLE13* interferes with *S. meliloti* NF synthesis. For this purpose, the NF-overproducing strain Gmi6390:2011 (pMH682; Roche et al., 1991) was inoculated on *35S:MtCLE12* and *35S:MtCLE13* transgenic roots (Supplemental Fig. S3). Similar to results obtained with the wild-type strain, nodulation was totally abolished but was unaffected on *35S:MtCLE4* and control *35S:GUS* roots.

To assess whether early NF signaling events still take place in roots ectopically overexpressing these *CLE* genes, we analyzed the transcription of the early marker, *ENOD11*, using a GUS transcriptional reporter (*pENOD11:GUS*) in *35S:MtCLE12* and *35S:MtCLE13* transgenic roots (Journet et al., 2001) and compared it with transgenic roots ectopically overexpressing either firefly luciferase (*LUC*) or *MtCLE4*. The transgenic roots were inoculated and stained with GUS at 3 dpi. In the *35S:LUC* and *35S:MtCLE4* transgenic roots, GUS staining was observed in the epidermal cells at sites of incipient infection (Fig. 7B) but not in *35S:MtCLE12* and *35S:MtCLE13* transgenic roots (Fig. 7B). These results suggest that ectopic expression of *MtCLE12* and *MtCLE13*, but not of *MtCLE4*, inhibits nodulation at the very early stages of NF signal transduction, before the onset of *ENOD11* expression.

Long-Distance Effects of *35S:MtCLE12* and *35S:MtCLE13* Transgenic Roots on Wild-Type Shoots

While analyzing the effects of *35S:MtCLE12* and *35S:MtCLE13* on the nodule number, we noticed that the petioles in these composite plants were longer than those in controls. To quantify this observation, we compared plants with *35S:MtCLE12*, *35S:MtCLE13*, and, as controls, *35S:GUS* and *35S:MtCLE4* transgenic roots. After growth in nitrogen-rich medium for 40 d after germination, the longest petiole on each plant was measured (Fig. 8A). For each construct, 60 plants were analyzed over three independent experiments. The average petiole length on control and *35S:MtCLE4* composite plants was 2.32 ± 0.36 and 2.21 ± 0.36 cm, respectively, whereas that on *35S:MtCLE12* and *35S:MtCLE13* composite plants was 3.06 ± 0.36 and 3.76 ±

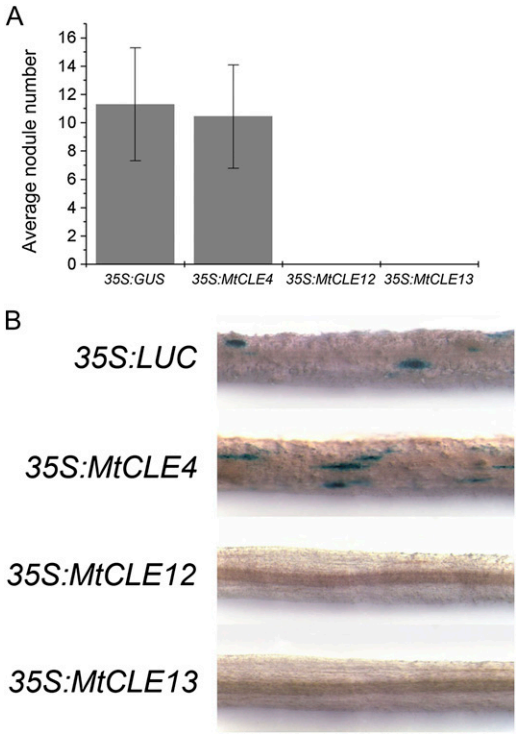

Figure 7. Inhibition of nodulation in *35S:MtCLE12* and *35S:MtCLE13* transgenic roots. A, Average nodule number on roots expressing *35S:GUS*, *35S:MtCLE4*, *35S:MtCLE12*, and *35S:MtCLE13* at 21 dpi ($n = 28$–66). Data and error bars represent means ± SD. B, *pMtENOD11:GUS* activity in roots expressing *35S:LUC*, *35S:GUS*, *35S:MtCLE12*, and *35S:MtCLE13* at 5 dpi. No staining is visible in the *35S:MtCLE12* and *35S:MtCLE13* samples.

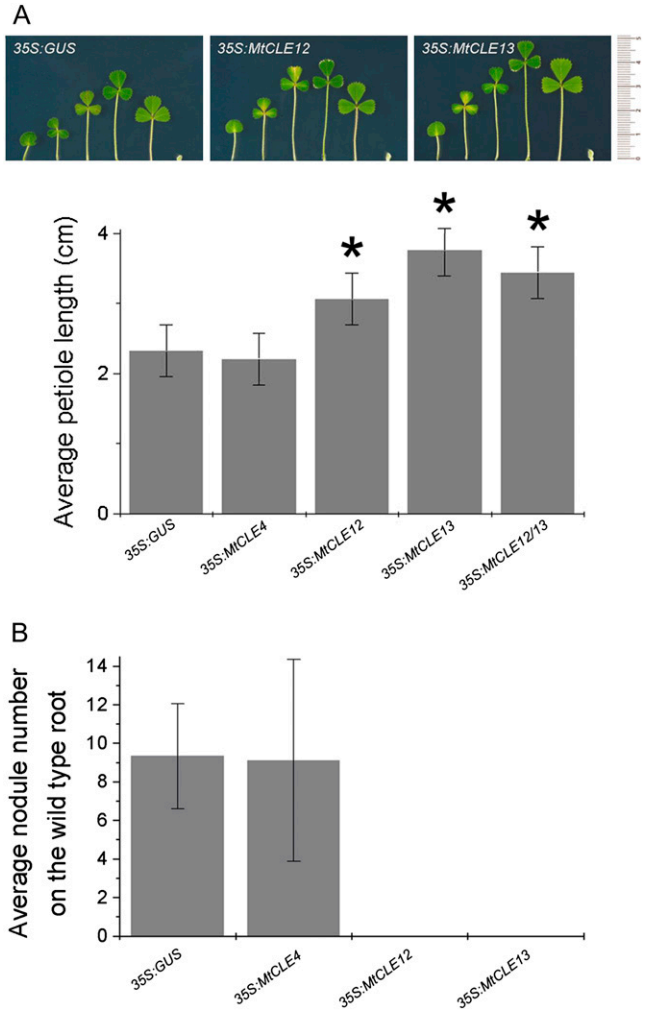

Figure 8. Long-distance effects of roots expressing *35S:MtCLE12* and *35S:MtCLE13* on petiole length and wild-type root nodulation of composite plants. A, Petioles of one 5-week-old composite plant with roots expressing *35S:GUS*, *35S:MtCLE12*, or *35S:MtCLE13*. The graph represents the average petiole lengths of composite plants carrying *35S:GUS*, *35S:MtCLE4*, *35S:MtCLE12*, *35S:MtCLE13*, or *35S:MtCLE12* and *35S:MtCLE13* transgenic roots at 4 weeks post germination ($n = 37–51$). Data and error bars represent means ± SE. Asterisks mark groups statistically different from the control (*35S:GUS*). B, Average nodule number at 7 dpi on the wild-type main roots of composite plants bearing additional transgenic *35S:GUS* ($n = 65$), *35S:MtCLE4* ($n = 10$), *35S:MtCLE12* ($n = 12$), or *35S:MtCLE13* ($n = 71$) roots. Data and error bars represent means ± SD. [See online article for color version of this figure.]

0.36 cm, respectively. To analyze whether ectopic expression of *MtCLE12* and *MtCLE13* would have a synergistic effect on the petioles of the wild-type shoot, composite plants were made carrying transgenic roots containing both *35S:MtCLE12* and *35S:MtCLE13* constructs (*35S:MtCLE12/13*). The average petiole length was 3.44 ± 0.36 cm, which is not statistically different from the petiole length measured on composite plants with the *35S:MtCLE13* construct alone (Fig. 8A). qRT-PCR was used to confirm the ectopic overexpression of each construct.

A longer petiole length could either indicate a specific effect of *MtCLE12* and *MtCLE13* on petiole growth or an overall faster development. To distinguish between these two hypotheses, developmental stages were assigned to each composite plant according to the method described by Bucciarelli et al. (2006). The results revealed no clear differences in the rate of composite plant development (Supplemental Fig. S4). However, plants with roots expressing *35S:MtCLE13* were out of the range of the control plants and, therefore, deemed to be a little faster in development. Leaf sizes of *35S:MtCLE12* and *35S:MtCLE13* composite plants, calculated with ImageJ (http://rsb.info.nih.gov/ij/), showed no statistically significant differences compared with controls.

Long-Distance Effects of *35S:MtCLE12* and *35S:MtCLE13* Transgenic Roots on Nodulation of Wild-Type Roots

In the *Agrobacterium rhizogenes* transgenic root assay, cotransformed transgenic roots were identified by screening for GFP roots (see "Materials and Methods"). Often, non-GFP-expressing roots grow on the same composite plant, suggesting that these roots are not cotransformed and contain only endogenous *A. rhizogenes* T-DNA(s). We repeatedly saw no nodules on these roots when the composite plants carried *35S:MtCLE12* and *35S:MtCLE13* transgenic roots. These observations indicated that the expression of *35S:MtCLE12* or *35S:MtCLE13* in roots might have a negative systemic effect on the nodulation of roots that do not express the constructs but grow on the same plant. Therefore, genomic DNA was prepared from GFP-fluorescent and nonfluorescent roots, and the presence of the *GFP* gene was analyzed by PCR. In some composite plants (Supplemental Fig. S5B), nonfluorescent roots still contained the *GFP* gene. Therefore, these observations did not unequivocally demonstrate a negative systemic influence of *35S:MtCLE12* or *35S:MtCLE13* on nodulation.

With a different procedure (see "Materials and Methods"), composite plants were generated with small transgenic roots while the wild-type root was kept intact. At 7 dpi with *Sm2011-GFP*, a Nod$^-$ phenotype was observed on the primary wild-type root of *35S:MtCLE12* and *35S:MtCLE13* composite plants (Fig. 8B), and on average nine nodules were counted on the primary wild-type roots of *35S:MtCLE4* and *35S:GUS* control plants. Given that plants were grown in an aeroponic system that confined the roots of all the plants in the same compartment, we can rule out that this phenotype is the result of peptide diffusion. These data show that ectopic overexpression of *MtCLE12* and *MtCLE13* abolishes nodulation not only locally in transgenic roots but also systemically in nontransformed roots of the same plant.

Analysis of the Long-Distance Responses in the *sunn-1* Mutant Background

Nodulation is under the control of AON, a systemic response that involves shoot-controlled factors (Magori

and Kawaguchi, 2009). Because of the long-distance responses observed when *MtCLE12* and *MtCLE13* are ectopically overexpressed, we investigated whether *MtCLE12* and *MtCLE13* are involved in AON and might be perceived by the SUNN receptor. Therefore, we tested whether the long-distance effects provoked by *35S:MtCLE13* expression on petiole length and on nodulation could be observed in the *sunn-1* mutant background (Schnabel et al., 2005).

In contrast to the results in the wild-type background, the petiole length did not elongate in composite *sunn-1* mutant plants containing roots expressing *35S:MtCLE13* (Fig. 9A). The average petiole length was 2.7 ± 0.7 cm, which is comparable to that of control plants (2.4 ± 0.7 cm; Fig. 9A).

On average, only 5.3 nodules occurred on *sunn-1,35S:MtCLE13*-transformed roots versus 49.0 nodules on the *sunn-1,35S:GUS* roots. The long-distance repression of nodulation was investigated in the *sunn-1* mutant background with the "hypocotyl-stabbing method" on plants growing under aeroponic conditions. Nodule numbers were counted at 7 dpi with *Sm2011-GFP*. Nontransformed primary roots of control plants had on average 74.0 nodules versus 17.6 nodules on the main root of *sunn-1* plants that expressed *35S:MtCLE13* in transgenic roots (Fig. 9C). Together, these analyses in the *sunn-1* mutant background revealed that the petiole elongation was SUNN dependent while the nodulation repression depended only partially on SUNN.

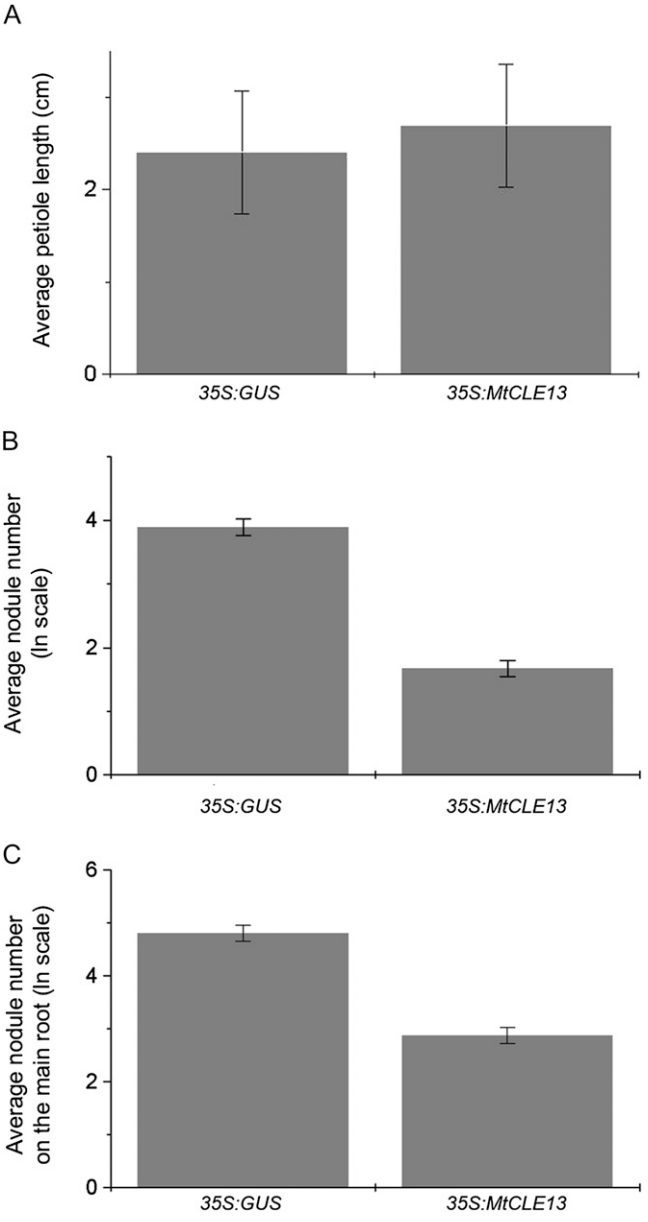

Figure 9. Local and systemic responses in the *sunn-1* mutant. A, Average length of the longest petiole of composite plants with roots ectopically expressing either *35S:GUS* or *35S:MtCLE13* at 4 weeks post germination ($n = 12$). Data and error bars represent means ± SE. B, The ln (logarithmus naturalis) of the nodule number at 7 dpi on *35S:GUS* or *35S:MtCLE13* transgenic roots ($n = 10–12$). C, The ln of the nodule number at 7 dpi on the wild-type main roots of plants bearing *35S:GUS* or *35S:MtCLE13* transgenic roots ($n = 17–24$). Data and error bars represent means ± SE.

DISCUSSION

CLE Family in *M. truncatula*

With specialized BLAST searches, 25 *MtCLE* genes were identified in the Mt2.0 release of the *M. truncatula* genome that represents approximately 60% of the genome, and more genes are expected upon completion of the genome sequencing. A more accurate picture of the size of the *CLE* gene family derives from the analysis of *L. japonicus* and Arabidopsis. The genome of *L. japonicus* is comparable in size to that of *M. truncatula* (470 Mb), and currently 91.3% of its genome has been sequenced. Thus far, 39 *CLE* genes have been identified in *L. japonicus* (Sato et al., 2008; Okamoto et al., 2009), which is equivalent to the 32 *CLE* genes in the completely sequenced Arabidopsis genome (157 Mb; Cock and McCormick, 2001; Oelkers et al., 2008).

qRT-PCR detection of 15 *MtCLE* transcripts revealed six to be expressed specifically in roots, three in shoots, one in nodules, and five across several tissues, hinting at CLE peptide involvement in a multitude of developmental processes throughout the plant (Mitchum et al., 2008). For the remaining 10 *MtCLE* genes, no transcripts were detected because either they are very lowly expressed and/or respond to specific biotic or abiotic stimuli or they have low abundant cell type-specific expression or are pseudogenes.

As we were interested in CLE peptide function during nodulation, *MtCLE12* and *MtCLE13* were selected for further analysis because they were up-regulated in nodulated roots. The CLE domain sequences of *MtCLE12* and *MtCLE13* are very similar, which is indicative of redundant functions, but the gene expression patterns, although partially overlapping, are

not identical. For instance, the *MtCLE13* expression is specific for nodulation, while *MtCLE12* transcripts occur also at low levels in root tips, cotyledons, and first leaves. Moreover, upon inoculation, the *MtCLE13* expression is up-regulated much earlier than that of *MtCLE12*. The promoter of *MtCLE13* functions in the NF-activated cortical cells; its activity is later restricted to the nodule primordium and is maintained through nodule maturity in the apical meristematic zone. In contrast, the *MtCLE12* promoter activity occurs first in young round nodules and, similar to that of *MtCLE13*, is later restricted to the apical zone. Finally, the expression of *MtCLE13* is induced rapidly by cytokinin, while that of *MtCLE12* is unaffected.

In the genome of *L. japonicus*, three *CLE* genes have been identified to be up-regulated by rhizobial inoculation (Okamoto et al., 2009). *LjCLE-RS1* and *LjCLE-RS2* have a high degree of similarity with the CLE domain of *MtCLE12* and *MtCLE13*, but no nodulation-related *MtCLE* gene was found with a CLE domain similar to that of *LjCLE3*. Interestingly, *LjCLE-RS1* and *LjCLE-RS2* are also up-regulated at early stages of nodulation. Based on sequence similarity and expression profiles, *MtCLE13* and *LjCLE-RS1/LjCLE-RS2* might exert a comparable function during indeterminate and determinate nodule development, respectively.

Studies on the putative CLE peptides of Arabidopsis (Ito et al., 2006; Ni and Clark, 2006; Strabala et al., 2006; Whitford et al., 2008) have shown a direct relationship between CLE domain sequence and induced phenotypes. MtCLE12 and MtCLE13 are most similar to a group of less characterized Arabidopsis CLE peptides (AtCLE1–AtCLE7) that are broadly produced with higher activity levels in the root (Sharma et al., 2003; Ito et al., 2006). Exogenous peptide addition did not suppress procambial-to-xylem cell transdifferentiation in a zinnia cell culture, while application of high, but not low, concentrations of peptides resulted in primary root meristem arrest (Ito et al., 2006; Strabala et al., 2006; Kinoshita et al., 2007; Whitford et al., 2008). Furthermore, ectopic overexpression of this group of peptides resulted in root elongation, mild *wus* loss-of-function phenotypes, mild distorted leaves, and dwarfing in later growth stages (Strabala et al., 2006). Upon exogenous peptide addition or ectopic overexpression in transgenic roots of *MtCLE12* and *MtCLE13*, neither root growth arrest nor enhanced root elongation was observed. Because root growth analysis of *A. rhizogenes*-generated roots is technically difficult, phenotypic analysis of transgenic plants carrying heritable *35S:MtCLE12* or *35S:MtCLE13* constructs might help to decipher whether these CLE peptides do indeed induce root growth defects. The CLE domain sequence of *MtCLE4* is most highly homologous to type I Arabidopsis CLE peptides, to which CLV3 belongs. This class of CLE peptides causes root meristem arrest upon exogenous application or ectopic overexpression. As expected, exogenous MtCLE4p application inhibited root growth by 24%.

Nodule-Related *MtCLE12* and *MtCLE13* Expression Is Linked with Differentiation and Dedifferentiation Processes

If *MtCLE13* were to be involved in nodulation, its transcription would depend on early nodulation signaling components. Quantitative detection of *MtCLE13* transcripts across different nodulation mutants revealed that functional DMI1, DMI2, DMI3, NSP1, NSP2, and NIN, but not ERN1, proteins are necessary for *MtCLE13* expression. Interestingly, the *ERN1* mutant, *bit1-1*, is the only mutant in which cell division is initiated and small arrested primordia are observed, indicative for active NF signaling toward the cortex and pericycle (Andriankaja et al., 2007; Middleton et al., 2007). *MtCLE13* transcript expression was quickly induced by cytokinin, but not by auxin, the former being the most important hormone for primordium initiation (Gonzalez-Rizzo et al., 2006; Murray et al., 2007; Tirichine et al., 2007). These data show that *MtCLE13* transcript expression is positioned downstream of early NF signaling components and suggest a role downstream of cytokinin perception in the control of organ development.

pMtCLE13:GUS analysis indicated that *MtCLE13* transcripts are expressed at very early stages of infection within nodulation-susceptible zones of the root cortex. The expression pattern is reminiscent of the signal gradient hypothesis, in which opposing signal gradients from the vasculature and from NF signaling at the epidermis would delimit the cellular landscape to form a nodule (Smit et al., 1995; Heidstra et al., 1997; van Spronsen et al., 2001). Because *MtCLE13* is induced by cytokinin, its expression pattern presumably reflects an internal cytokinin gradient in the cortex. Consequently, MtCLE13 peptides might serve as subsequent intercellular signals to control downstream responses. Once cell division was initiated, *MtCLE13* expression was the strongest in the dividing cortical and pericycle cells. CLE peptides have been shown to regulate the balance between cell division and differentiation (Ito et al., 2006; Kondo et al., 2006; Simon and Stahl, 2006; Whitford et al., 2008). Therefore, the MtCLE13 peptide gradient might maintain cell division and/or cell identity during the course of nodule development. Analysis of downstream responses to MtCLE13 peptide overexpression via genome-wide expression analysis might provide further insight into MtCLE13 function.

The expression of *MtCLE12* is also correlated with cell division and differentiation. Expression of *MtCLE12* during nodule development was first observed throughout the mature primordium, where *MtCLE13* expression also was detected. The late expression pattern of *MtCLE12* was confirmed by the absence of expression in the inoculated nodulation mutants, because none of the tested mutants developed nodule primordia of a stage corresponding with the *MtCLE12* expression. By which trigger *MtCLE12* expression is induced is thus far unknown, but application

of neither cytokinin nor auxin could activate *MtCLE12* expression. The transcription factor *MtHAP2-1*, located in nodule meristematic tissues, is essential for meristem differentiation (Combier et al., 2006). It would be interesting to determine whether a functional *MtHAP2-1* is necessary for *MtCLE12* induction or whether *MtCLE12* regulates *MtHAP2-1* expression.

In mature nodules, both *MtCLE12* and *MtCLE13* are expressed apically, in a zone comprising meristematic cells and cells of the early infection zone. In some nodules, *MtCLE13* expression was higher in the provascular strands of the nodule meristem than in other meristematic cell types. Expression of *MtCLE12* and *MtCLE13* in the nodule apex again suggests a regulatory role for their encoded peptides in nodule meristem cell proliferation and/or differentiation.

MtCLE12, *MtCLE13*, or a Peptide with a Related Sequence Might Control Nodule Number

The lack of nodule development in transgenic roots ectopically overexpressing either *MtCLE12* or *MtCLE13* hints at a role for CLE signaling in controlling nodule number. Nodulation on *35S*:*MtCLE12* and *35S*:*MtCLE13*, but not on *35S*:*MtCLE4*, roots was totally abolished at the level of NF perception: no *MtENOD11* expression and no developing nodules were seen upon inoculation of transgenic roots. This suppressive effect on nodulation was not phenocopied by exogenous application of synthetic peptides. One possible reason could be related to a role for post-translational hydroxyprolination and subsequent arabinosylation on CLE peptide bioactivity, as suggested for Arabidopsis CLE peptides AtCLE1 to AtCLE7 (Strabala et al., 2006; Ohyama et al., 2009). Moreover, CLV3 arabinosylation has been found to be critical for high-affinity binding to the CLV1 ectodomain (Ohyama et al., 2009).

Nodule number is controlled by different processes. Our results suggest that CLE peptides are specifically involved in AON because nodule development was inhibited systemically in wild-type roots of composite plants containing roots ectopically overexpressing either *MtCLE12* or *MtCLE13*. Moreover, ectopic expression of *MtCLE12* and *MtCLE13* in roots promoted petiole elongation in wild-type shoots of these composite plants. Taken together, these results demonstrate that MtCLE12 and MtCLE13 peptides can activate physiological responses at significant distances from the site of transgene expression. In the *sunn-1* mutant background, no petiole elongation was observed, but the nodule number was strongly suppressed instead of a complete nodule development inhibition, like that observed in wild-type primary roots. The *sunn-1* mutant might possess residual SUNN activity that could potentially allow MtCLE12 or MtCLE13 perception and downstream signaling at a level sufficient for only a mild suppression of nodulation but insufficient for promotion of petiole elongation. The ectopic expression of *LjCLE-RS1* or *LjCLE-RS2* of *L. japonicus* strongly reduces nodulation locally and systemically (Okamoto et al., 2009). This inhibitive effect on nodulation was abolished in the *hypernodulating1-4* (*har1-4*) mutant roots, *HAR1* being an orthologous gene to *SUNN* (Okamoto et al., 2009). The phenotypic differences between mutants could potentially be attributed to differences in allele functionality, because *har1-4* bears a missense mutation in the LRR ectodomain and *sunn-1* is mutated in the kinase domain (Kawaguchi et al., 2002; Krusell et al., 2002; Nishimura et al., 2002; Schnabel et al., 2005). Accordingly, a missense mutation in the LRR ectodomain of CLV1 has a stronger phenotype than a mutation in the kinase domain (Diévart et al., 2003). Moreover, the *har1-4* mutant allele causes a more severe nodulation phenotype than the *har1-5* allele, which is mutated in the intracellular kinase domain (Kawaguchi et al., 2002; Krusell et al., 2002; Nishimura et al., 2002; Schnabel et al., 2005). Thus, the differences in phenotype might simply be due to residual activities of the mutant protein or to a potentially dominant negative effect on interacting receptors, as for mutant alleles of CLV1 (Diévart et al., 2003).

Because SUNN belongs to class XI of LRR-RLKs, to which a few CLE peptide receptors belong (PXY/TDR and CLV1), it is tempting to propose that SUNN might be part of the receptor complex for MtCLE12 or MtCLE13. However, grafting studies have shown that SUNN and its orthologs are active in the shoot to invoke AON via a shoot-localized mechanism (Nutman, 1952; Delves et al., 1986; Krusell et al., 2002; Nishimura et al., 2002; Searle et al., 2003; Schnabel et al., 2005). Consequently, if the MtCLE12 and MtCLE13 peptides, which are produced upon nodulation in the root, could be perceived by SUNN, long-distance root-to-shoot translocation of the peptides would have to occur, which is in contradiction to the short-distance signaling activities proposed for many CLE peptides (Fukuda et al., 2007; Hirakawa et al., 2008; Whitford et al., 2008; Miwa et al., 2009; Stahl et al., 2009).

Alternatively, the various CLE peptide bioactivities observed upon ectopic overexpression of *MtCLE12* or *MtCLE13* in roots might mimic the signaling of structurally related CLE peptides that are produced in the shoot, the place of action of SUNN and its orthologs. Because the strong *35S* promoter is expressed in the root vasculature, the ectopically produced CLE peptides might be systemically spread throughout the plant and be perceived by the SUNN protein in the shoot. As the SUNN proteins might also be produced in the root vasculature (Schnabel et al., 2005; Nontachaiyapoom et al., 2007), we cannot rule out that the misexpressed CLE proteins in the root vasculature are locally perceived by SUNN to provoke the observed long-distance effects. The shoot-expressed *CLE* gene might be *MtCLE12* itself, because expression analysis has revealed that *MtCLE12* is also expressed in first leaves and cotyledons, the site of SUNN activity. In this scenario, *MtCLE12* and *MtCLE13* activity

within the nodule would not be linked with AON but rather with balancing proliferation and differentiation, as supported by the observed expression patterns.

It is equally possible that *MtCLE12* and *MtCLE13* perception occurs locally in the root, resulting in secondary signals that travel to the shoot, where they are recognized to provoke AON and petiole elongation. Interestingly, the expression of *MtCLE12* and *MtCLE13* coincides with the activation and progression of AON that is first initiated when the first nodule primordia are formed and is strengthened as more nodules develop (Nutman, 1952; Delves et al., 1986; Takats, 1990; Wopereis et al., 2000; Krusell et al., 2002; Nishimura et al., 2002; Searle et al., 2003; Schnabel et al., 2005; Li et al., 2009). Besides the long-distance effect on nodulation, *35S:MtCLE12* and *35S:MtCLE13* transgenic roots induced elongation of the petioles of the composite plants. Insights into petiole growth might hint at downstream responses of *MtCLE12* and *MtCLE13* signaling. Petiole length elongation is influenced by auxin, ethylene, abscisic acid, and gibberellins (Cox et al., 2004; Millenaar et al., 2009; Pierik et al., 2009).

In conclusion, CLE peptides most probably play different roles in nodulation. Expression patterns hint at roles during cellular differentiation processes, both at the onset of nodulation and later during nodule meristem development and subsequent homeostasis. Moreover, intertwined or not, the functional analyses imply a role for *MtCLE* peptides in AON. In Arabidopsis, the CLE peptide signaling is intricate and mediated by different receptor complexes (Miwa et al., 2009; Stahl et al., 2009). In silico analysis of the *M. truncatula* genome has revealed additional genes that belong to class XI of LRR-RLKs, and expression profiling indicates that they are up-regulated in the nodule. Future studies will investigate the individual role of each of these peptides and their corresponding receptors during the nodulation process and will provide valuable insight into nodule development, nodule cell type determination, and regulation of nodule number.

MATERIALS AND METHODS

Biological Material

Medicago truncatula 'Jemalong A17' and 'J5' as well as *nin*, *bit1-1*, *nsp1*, *nsp2*, *dmi1*, *dmi2*, *dmi3*, and *sunn-1* mutants (Catoira et al., 2000; Oldroyd and Long, 2003; Marsh et al., 2007; Middleton et al., 2007) and *pENOD11:GUS* transgenic seeds (Journet et al., 2001) were grown and inoculated as described (Mergaert et al., 2003). *Sinorhizobium meliloti 1021*, *Sm1021* pHC60-GFP (Cheng and Walker, 1998), *Sm1021* pQE81-dsRedT3 (Bevis and Glick, 2002), *Sm2011* pBHR-mRFP (Smit et al., 2005), *Sm2011* pHC60-GFP (Cheng and Walker, 1998), and *Sm2011* pMH682-Gmi6390 (Roche et al., 1991) were grown at 28°C in yeast extract broth medium (Vervliet et al., 1975) supplemented with 10 mg L^{-1} tetracycline for the *Sm1021* pHC60-GFP, *Sm1021* pQE81-dsRedT3, *Sm2011* pBHR-mRFP, *Sm2011* pHC60-GFP, and *Sm1021* pMH682-Gmi6390 strains.

PCR fragments corresponding to the full-length open reading frames of *MtCLE4*, *MtCLE12*, and *MtCLE13* were amplified from *M. truncatula* cDNA and cloned in pB7WG2D driven by the cauliflower mosaic virus 35S promoter (De Loose et al., 1995; Karimi et al., 2002). The vector pK7m34GW2-8m21GW3D was used for the simultaneous ectopic expression of *MtCLE12* and *MtCLE13* (Karimi et al., 2007). For *promoter:GUS* analysis, a 2-kb region upstream of *MtCLE12* and *MtCLE13* was isolated from genomic DNA based on the available genomic data (http://www.ncbi.nlm.nih.gov/). The promoters were fused to the *uidA* gene in pKm43GWRolDC1 (Karimi et al., 2002). Primers used for amplification are presented in Supplemental Table S3.

For the qRT-PCR analysis, *M. truncatula* J5 plants were grown in vitro in square petri dishes (12 × 12 cm) on nitrogen-poor SOLi agar (Blondon, 1964). Root tips, SAMs, cotyledons, and first leaves were harvested after 7d; mature leaves, stems, and roots from plants grown in perlite and watered with nitrogen-poor SOLi medium after 1 month; and nodulated roots from plants inoculated with *Sm1021* pHC60-GFP after 1 month. For the analysis of temporal expression during nodulation, nodules were obtained 4 to 10 dpi from plants grown in pouches, watered with nitrogen-poor SOLi medium, and inoculated with *Sm1021* pHC60-GFP. Infection threads were visible from 4 dpi on, nodule primordia at 6 dpi, and small nodules at 8 dpi. Two days later, at 10 dpi, slightly bigger nodules were observed. Tissue was collected by visualizing the green fluorescent bacteria with a MZFLII stereomicroscope (Leica Microsystems) equipped with a blue light source and a Leica GFP Plus filter set (λ_{ex} = 480/40, λ_{em} = 510 nm LP barrier filter). Zone I of uninoculated roots was isolated at the same developmental stage as the 4-dpi stage.

In Silico Identification of *M. truncatula CLE* Genes

BLAST searches were done at The Institute for Genomic Research (www.tigr.org/tdb/tgi/) or at the National Center for Biotechnology Information (www.ncbi.nlm.nih.gov/BLAST/). The CLE family was identified by repetitive searches similar to those conducted by Cock and McCormick (2001). Repetitive searches were done with the Medicago Gene Index (MGI) at the Dana-Farber Cancer Institute (release 9.0) first with the tBLASTn PAM30 algorithm for the Arabidopsis CLE box consensus (RXXPXXPXPXH). The first identified sequence, MtCLE1 (GenBank EST AW586793), which was confirmed to encode a MtCLE-like peptide, was based on the predicted peptide length (less than 150 amino acids), the presence of a C-terminally localized CLE box, and an N-terminal signal peptide as predicted by HMM SignalP and neural networks (Bendtsen et al., 2004). This first sequence was used to repeat the same search, each time with an additional homologous CLE box sequence, until no unknown family members were found in the EST data. These CLE box sequences were used in the same iterative BLAST searches to identify additional putative CLE peptides from the partially completed genomic sequence (Mt2.0). Sequences were aligned with AlignX within the VectorNTI Advance version 10 suite of programs (http://www.invitrogen.com).

RNA Extraction, cDNA Synthesis, and qRT-PCR Analysis

Total RNA was isolated with the RNeasy Plant Mini Kit (Qiagen) according to the manufacturer's instructions. After a DNase treatment, the samples were purified through NH_4Ac (5 M) precipitation, quality controlled, and quantified with a Nanodrop spectrophotometer (Isogen). RNA (2 μg) was used for cDNA synthesis with the SuperScript Reverse Transcriptase Kit (Invitrogen). The samples were diluted 50 times and stored at −20°C until further use. The qRT-PCR experiments were done on a LightCycler 480 (Roche Diagnostics), and SYBR Green was used for detection. All reactions were done in triplicate and averaged. The total reaction volume was 5 μL (2.5 μL of master mix, 0.25 μL [5 μM] of each primer, and 2 μL of cDNA). Cycle threshold values were obtained with the accompanying software, and data were analyzed with the $2^{-\Delta\Delta Ct}$ method (Livak and Schmittgen, 2001). The relative expression was normalized against the constitutively expressed 40S ribosomal S8 protein (TC100533; MGI). Primers used (Supplemental Table S3) were unique in the MGI version 9.0 and the Medicago EST Navigation System databases (Journet et al., 2002). Each experiment was repeated at least three times with independent biological tissue.

Statistical Analysis

To estimate the genotype effects on developmental stage, petiole length, and root length, the linear mixed model (random terms underlined) $y = \mu +$ genotype + $\underline{\text{experiment}} + \varepsilon$ was fitted to the data, where y represents the variable, μ is the overall mean, genotype is the fixed genotype effect, $\underline{\text{experiment}}$ represents random experimental effects, and ε is the random error. Statistical significance of genotype effects was assessed by a Wald test. In

the case of the nodule number in *sunn-1* plants, a generalized linear mixed model, of the form $y = \mu$ + genotype + experiment + ε with a Poisson distribution and a logarithmic link, was fitted to the data. Again, the statistical significance of genotype effects was assessed by a Wald test. All analyses were done with Genstat (http://www.vsni.co.uk/software/genstat/).

In Vitro Application of MtCLE Synthetic Peptides, Auxins, and Cytokinins

Peptides (AGAMOUS, APNNHHYSSAGRQDQT; MtCLE4, KRGVpSGANPLHNR; MtCLE12, DRLSpGGpNHIHN; and MtCLE13, DRLSpAGpDPQHNG; lowercase p indicates hydroxylated Pro), with a purity greater than 89% (ServiceXS), were dissolved in a filter-sterilized sodium phosphate buffer (pH 6, 50 mM [43.5 mM NaH_2PO_4 and 6.2 mM Na_2HPO_4]). Two-day-old Jemalong J5 seedlings were grown in vitro in square petri dishes (12 × 12 cm) on agar HP 696-7470 (Kalys) containing the SOLi medium supplemented with 1 mM NH_4NO_3 and 10 μM peptides (Fiers et al., 2005). The plants were cultured at 25°C with a 16-h photoperiod and 70 μE m^{-2} m^{-1} light intensity per day. The roots were covered with aluminum foil for light protection. After 8 d of growth, the root length of 16 plants under each condition was measured from the root tip of the primary root to the base of the hypocotyls with the ImageJ 1.40b program (http://rsb.info.nih.gov/ij/). The experiment was repeated three times with comparable results.

Auxins (10^{-6} IAA) and cytokinins (10^{-7} BAP) were diluted in dimethyl sulfoxide and supplemented to the medium of 5-d-old, in vitro-grown plants. As a control, plants were grown without supplemented hormones. The growth conditions of the seedlings were the same as above. After 0, 3, 6, 12, and 24 h of incubation, the roots of 18 plants under each condition were harvested and analyzed by qRT-PCR. The experiment was repeated twice with comparable results.

Agrobacterium rhizogenes-Mediated Transgenic Root Transformation

The protocol was adapted from Boisson-Dernier et al. (2001). Approximately 48 h after germination, the radicle was sectioned at 5 mm from the root tip with a sterile scalpel. Sectioned seedlings were infected by coating the freshly cut surface with the binary vector-containing *A. rhizogenes* Arqua1 strains. The *A. rhizogenes* strain was grown at 28°C for 2 d on solid yeast extract broth medium with the appropriate antibiotics (Quandt et al., 1993). The infected seedlings were placed on agar (Kalys) containing the SOLi medium supplemented with 1 mM NH_4NO_3, in square petri dishes (12 × 12 cm) placed vertically for 5 d at 20°C with a 16-h photoperiod and light at 70 μE m^{-2} s^{-1}. Subsequently, plants were placed on the same medium between brown paper at 25°C and under identical light conditions. One and 2 weeks later, plants were screened for transgenic roots and characterized by GFP fluorescence with a MZFLII stereomicroscope (Leica Microsystems) equipped with a blue light source and a Leica GFP Plus filter set. One main transgenic root was retained per composite plant. Four weeks after infection, plants were transferred to an aeroponic system, pouches, or perlite-containing pots and incubated with SOLi medium. Three to 7 d after planting, composite plants were inoculated. The petiole lengths were measured on plants grown under the same conditions but incubated with nitrogen-containing ISV medium (E.-P. Journet, D. Barker, M. Harrison, and E. Kondorosi, unpublished data). Forty days after germination, the longest petiole of each plant was scored by ImageJ (http://rsb.info.nih.gov/ij/).

In some experiments, the main root was kept on the juvenile plant and infected by stabbing the hypocotyls with a fine needle containing an *A. rhizogenes* culture and cotransformed as described above, after which the plants were grown for 2 weeks at 25°C with a 16-h photoperiod and light at 70 μE m^{-2} s^{-1}. After the plants had been transferred to an aeroponic system for 7 d, nodulation was analyzed on the main, untransformed root of plants bearing GFP-positive hairy roots.

Histochemical Localization of GUS Activity

GUS activity in cotransformed roots and nodules was analyzed with 5-bromo-4-chloro-3-indolyl-β-D-glucuronic acid as substrate (Van den Eede et al., 1992). Roots and nodules were vacuum infiltrated during 20 min and subsequently incubated in GUS buffer at 37°C. Incubation lasted 3.5 and 7 h for *pMtCLE13-GUS* and *pMtCLE12-GUS*, respectively. After staining, root nodules were fixed, dehydrated, embedded with the Technovit 7100 kit (Heraeus Kulzer) according to the manufacturer's instructions, and sectioned with a microtome (Reichert-Jung). The 3-μm-thick sections were mounted on coated slides (Sigma-Aldrich). For tissue-specific staining, sections were submerged in a 0.05% (w/v) ruthenium red solution (Sigma-Aldrich), washed in distilled water, and dried. Finally, sections were mounted with Depex (BDH Chemicals). Photographs were taken with a Diaplan microscope equipped with bright- and dark-field optics (Leitz). GUS activity of *pENOD11*:*GUS* roots was visualized after 7 h of incubation.

In Situ Hybridization

Ten-micrometer sections of paraffin-embedded nodules were hybridized as described (Goormachtig et al., 1997). Nodules were harvested, incubated in fixation buffer, and maintained twice for 15 min under vacuum. A ^{35}S-labeled antisense probe against the complete open reading frame of *MtCLE13* was produced according to standard procedures (Sambrook et al., 1989). The probe was cloned into pBluescript KS+ (Stratagene) and further digested with *Hin*dIII restriction enzyme to yield templates for radioactive antisense probe production with T3 RNA polymerase (Invitrogen).

Supplemental Data

The following materials are available in the online version of this article.

Supplemental Figure S1. Sequence alignment of the *MtCLE* genes.

Supplemental Figure S2. *MtCLE13* transcript accumulation in mature nodules by in situ hybridization.

Supplemental Figure S3. Average nodule number on roots ectopically expressing *GUS*, *MtCLE4*, *MtCLE12*, or *MtCLE13* at 11 dpi with a NF-overproducing *S. meliloti* strain.

Supplemental Figure S4. Log10 of the developmental stage of composite plants carrying roots ectopically expressing *GUS*, *MtCLE4*, *MtCLE12*, *MtCLE13*, or *MtCLE12* and *MtCLE13*.

Supplemental Figure S5. Detailed genotypic analysis of transgenic roots obtained by *A. rhizogenes* transformation.

Supplemental Table S1. *MtCLE* identification.

Supplemental Table S2. Comparison of the CLE peptide sequences of *MtCLE4*, *MtCLE12*, and *MtCLE13* with the CLE peptide sequences from Arabidopsis *CLE* genes and from *LjCLE-RS1*, *LjCLE-RS2*, and *LjCLE3*.

Supplemental Table S3. Primers used in the analysis.

ACKNOWLEDGMENTS

We thank René Geurts (Wageningen University), Pascal Gamas and Clare Gough (Institut de la Recherche Agronomique-Toulouse), Doug Cook (University of California, Davis), and Giles Oldroyd (John Innes Institute) for *S. meliloti* strains and *M. truncatula* mutants, and our colleagues Annick De Keyser and Christa Verplancke for skillful technical assistance, Lorin Spruyt, Katja Katzer, Assia Saltykova, and Jorik Verbiest for their input during their master projects and theses, Wilson Ardiles for sequence analysis, Marnik Vuylsteke for help with the statistical analysis, Giel Van Noorden for critical reading of the manuscript, and Martine De Cock and Karel Spruyt for help in preparing the paper and figures, respectively.

Received January 21, 2010; accepted March 23, 2010; published March 26, 2010.

LITERATURE CITED

Andriankaja A, Boisson-Dernier A, Frances L, Sauviac L, Jauneau A, Barker DG, de Carvalho-Niebel F (2007) AP2-ERF transcription factors mediate Nod factor-dependent Mt *ENOD11* activation in root hairs via a novel *cis*-regulatory motif. Plant Cell **19:** 2866–2885

Bendtsen JD, Nielsen H, von Heijne G, Brunak S (2004) Improved prediction of signal peptides: SignalP 3.0. J Mol Biol **340:** 783–795

Bevis BJ, Glick BS (2002) Rapidly maturing variants of the *Discosoma* red fluorescent protein (DsRed). Nat Biotechnol **20:** 83–87

Blondon F (1964) Contribution à l'étude du développement de graminées fourragères: ray-grass et dactyle. Rev Gen Bot **71:** 293–381

Boisson-Dernier A, Chabaud M, Garcia F, Bécard G, Rosenberg C, Barker DG (2001) *Agrobacterium rhizogenes*-transformed roots of *Medicago truncatula* for the study of nitrogen-fixing and endomycorrhizal symbiotic associations. Mol Plant Microbe Interact **14:** 695–700

Boot KJM, van Brussel AAN, Tak T, Spaink HP, Kijne JW (1999) Lipochitin oligosaccharides from *Rhizobium leguminosarum* bv. *viciae* reduce auxin transport capacity in *Vicia sativa* subsp. *nigra* roots. Mol Plant Microbe Interact **12:** 839–844

Borisov AY, Madsen LH, Tsyganov VE, Umehara Y, Voroshilova VA, Batagov AO, Sandal N, Mortensen A, Schauser L, Ellis N, et al (2003) The *Sym35* gene required for root nodule development in pea is an ortholog of *Nin* from *Lotus japonicus*. Plant Physiol **131:** 1009–1017

Bucciarelli B, Hanan J, Palmquist D, Vance CP (2006) A standardized method for analysis of *Medicago truncatula* phenotypic development. Plant Physiol **142:** 207–219

Catoira R, Galera C, de Billy F, Penmetsa RV, Journet E-P, Maillet F, Rosenberg C, Cook D, Gough C, Dénarié J (2000) Four genes of *Medicago truncatula* controlling components of a Nod factor transduction pathway. Plant Cell **12:** 1647–1665

Cheng H-P, Walker GC (1998) Succinoglycan is required for initiation and elongation of infection threads during nodulation of alfalfa by *Rhizobium meliloti*. J Bacteriol **180:** 5183–5191

Clark SE, Williams RW, Meyerowitz EM (1997) The *CLAVATA1* gene encodes a putative receptor kinase that controls shoot and floral meristem size in Arabidopsis. Cell **89:** 575–585

Cock JM, McCormick S (2001) A large family of genes that share homology with *CLAVATA3*. Plant Physiol **126:** 939–942

Combier J-P, Frugier F, de Billy F, Boualem A, El-Yahyaoui F, Moreau S, Vernié T, Ott T, Gamas P, Crespi M, et al (2006) *MtHAP2-1* is a key transcriptional regulator of symbiotic nodule development regulated by microRNA169 in *Medicago truncatula*. Genes Dev **20:** 3084–3088

Cox MCH, Benschop JJ, Vreeburg RAM, Wagemaker CAM, Moritz T, Peeters AJM, Voesenek LACJ (2004) The roles of ethylene, auxin, abscisic acid, and gibberellin in the hyponastic growth of submerged *Rumex palustris* petioles. Plant Physiol **136:** 2948–2960

De Loose M, Danthinne X, Van Bockstaele E, Van Montagu M, Depicker A (1995) Different 5′ leader sequences modulate β-glucuronidase accumulation levels in transgenic *Nicotiana tabacum* plants. Euphytica **85:** 209–216

Delves AC, Mathews A, Day DA, Carter AS, Carroll BJ, Gresshoff PM (1986) Regulation of the soybean-*Rhizobium* nodule symbiosis by shoot and root factors. Plant Physiol **82:** 588–590

DeYoung BJ, Bickle KL, Schrage KJ, Muskett P, Patel K, Clark SE (2006) The CLAVATA1-related BAM1, BAM2 and BAM3 receptor kinase-like proteins are required for meristem function in Arabidopsis. Plant J **45:** 1–16

DeYoung BJ, Clark SE (2008) BAM receptors regulate stem cell specification and organ development through complex interactions with CLAVATA signaling. Genetics **180:** 895–904

Diévart A, Dalal M, Tax FE, Lacey AD, Huttly A, Li J, Clark SE (2003) *CLAVATA1* dominant-negative alleles reveal functional overlap between multiple receptor kinases that regulate meristem and organ development. Plant Cell **15:** 1198–1211

Ding Y, Oldroyd GED (2009) Positioning the nodule, the hormone dictum. Plant Signal Behav **4:** 89–93

Etchells JP, Turner SR (2010) The PXY-CLE41 receptor ligand pair defines a multifunctional pathway that controls the rate and orientation of vascular cell division. Development **137:** 767–774

Fiers M, Golemiec E, Xu J, van der Geest L, Heidstra R, Stiekema W, Liu C-M (2005) The 14-amino acid CLV3, CLE19, and CLE40 peptides trigger consumption of the root meristem in *Arabidopsis* through a *CLAVATA2*-dependent pathway. Plant Cell **17:** 2542–2553

Fisher K, Turner S (2007) PXY, a receptor-like kinase essential for maintaining polarity during plant vascular-tissue development. Curr Biol **17:** 1061–1066

Frugier F, Kosuta S, Murray JD, Crespi M, Szczyglowski K (2008) Cytokinin: secret agent of symbiosis. Trends Plant Sci **13:** 115–120

Fukuda H, Hirakawa Y, Sawa S (2007) Peptide signaling in vascular development. Curr Opin Plant Biol **10:** 477–482

Gleason C, Chaudhuri S, Yang T, Muñoz A, Poovaiah BW, Oldroyd GED (2006) Nodulation independent of rhizobia induced by a calcium-activated kinase lacking autoinhibition. Nature **441:** 1149–1152

Gonzalez-Rizzo S, Crespi M, Frugier F (2006) The *Medicago truncatula* CRE1 cytokinin receptor regulates lateral root development and early symbiotic interaction with *Sinorhizobium meliloti*. Plant Cell **18:** 2680–2693

Goormachtig S, Alves-Ferreira M, Van Montagu M, Engler G, Holsters M (1997) Expression of cell cycle genes during *Sesbania rostrata* stem nodule development. Mol Plant Microbe Interact **10:** 316–325

Heidstra R, Yang WC, Yalcin Y, Peck S, Emons A, van Kammen A, Bisseling T (1997) Ethylene provides positional information on cortical cell division but is not involved in Nod factor-induced root hair tip growth in *Rhizobium*-legume interaction. Development **124:** 1781–1787

Hirakawa Y, Shinohara H, Kondo Y, Inoue A, Nakanomyo I, Ogawa M, Sawa S, Ohashi-Ito K, Matsubayashi Y, Fukuda H (2008) Non-cell-autonomous control of vascular stem cell fate by a CLE peptide/receptor system. Proc Natl Acad Sci USA **105:** 15208–15213

Ito Y, Nakanomyo I, Motose H, Iwamoto K, Sawa S, Dohmae N, Fukuda H (2006) Dodeca-CLE peptides as suppressors of plant stem cell differentiation. Science **313:** 842–845

Jones KM, Kobayashi H, Davies BW, Taga ME, Walker GC (2007) How rhizobial symbionts invade plants: the *Sinorhizobium-Medicago* model. Nat Rev Microbiol **5:** 619–633

Journet E-P, El-Gachtouli N, Vernoud V, de Billy F, Pichon M, Dedieu A, Arnould C, Morandi D, Barker DG, Gianinazzi-Pearson V (2001) *Medicago truncatula ENOD11*: a novel RPRP-encoding early nodulin gene expressed during mycorrhization in arbuscule-containing cells. Mol Plant Microbe Interact **14:** 737–748

Journet E-P, van Tuinen D, Gouzy J, Crespeau H, Carreau V, Farmer M-J, Niebel A, Schiex T, Jaillon O, Chatagnier O, et al (2002) Exploring root symbiotic programs in the model legume *Medicago truncatula* using EST analysis. Nucleic Acids Res **30:** 5579–5592

Jun JH, Fiume E, Fletcher JC (2008) The CLE family of plant polypeptide signaling molecules. Cell Mol Life Sci **65:** 743–755

Karimi M, Bleys A, Vanderhaeghen R, Hilson P (2007) Building blocks for plant gene assembly. Plant Physiol **145:** 1183–1191

Karimi M, Inzé D, Depicker A (2002) GATEWAY™ vectors for *Agrobacterium*-mediated plant transformation. Trends Plant Sci **7:** 193–195

Kawaguchi M, Imaizumi-Anraku H, Koiwa H, Niwa S, Ikuta A, Syono K, Akao S (2002) Root, root hair, and symbiotic mutants of the model legume *Lotus japonicus*. Mol Plant Microbe Interact **15:** 17–26

Kinoshita A, Nakamura Y, Sasaki E, Kyozuka J, Fukuda H, Sawa S (2007) Gain-of-function phenotypes of chemically synthetic CLAVATA3/ESR-related (CLE) peptides in *Arabidopsis thaliana* and *Oryza sativa*. Plant Cell Physiol **48:** 1821–1825

Kondo T, Sawa S, Kinoshita A, Mizuno S, Kakimoto T, Fukuda H, Sakagami Y (2006) A plant peptide encoded by *CLV3* identified by in situ MALDI-TOF MS analysis. Science **313:** 845–848

Kosslak RM, Bohlool BB (1984) Suppression of nodule development of one side of a split-root system of soybeans caused by prior inoculation of the other side. Plant Physiol **75:** 125–130

Krusell L, Madsen LH, Sato S, Aubert G, Genua A, Szczyglowski K, Duc G, Kaneko T, Tabata S, de Bruijn F, et al (2002) Shoot control of root development and nodulation is mediated by a receptor-like kinase. Nature **420:** 422–426

Li D, Kinkema M, Gresshoff PM (2009) Autoregulation of nodulation (AON) in *Pisum sativum* (pea) involves signalling events associated with both nodule primordia development and nitrogen fixation. J Plant Physiol **166:** 955–967

Livak KJ, Schmittgen TD (2001) Analysis of relative gene expression data using real-time quantitative PCR and the $2^{-\Delta\Delta C_T}$ method. Methods **25:** 402–408

Madsen EB, Madsen LH, Radutoiu S, Olbryt M, Rakwalska M, Szczyglowski K, Sato S, Kaneko T, Tabata S, Sandal N, et al (2003) A receptor kinase gene of the LysM type is involved in legume perception in rhizobial signals. Nature **425:** 637–640

Magori S, Kawaguchi M (2009) Long-distance control of nodulation: molecules and models. Mol Cells **27:** 129–134

Marsh JF, Rakocevic A, Mitra RM, Brocard L, Sun J, Eschstruth A, Long SR, Schultze M, Ratet P, Oldroyd GED (2007) *Medicago truncatula NIN* is essential for rhizobial-independent nodule organogenesis induced

by autoactive calcium/calmodulin-dependent protein kinase. Plant Physiol **144:** 324–335

Mathesius U, Schlaman HRM, Spaink HP, Sautter C, Rolfe BG, Djordjevic MA (1998) Auxin transport inhibition precedes root nodule formation in white clover roots and is regulated by flavonoids and derivatives of chitin oligosaccharides. Plant J **14:** 23–34

Mergaert P, Nikovics K, Kelemen Z, Maunoury N, Vaubert D, Kondorosi A, Kondorosi E (2003) A novel family in *Medicago truncatula* consisting of more than 300 nodule-specific genes coding for small, secreted polypeptides with conserved cysteine motifs. Plant Physiol **132:** 161–173

Middleton PH, Jakab J, Penmetsa RV, Starker CG, Doll J, Kaló P, Prabhu R, Marsh JF, Mitra RM, Kereszt A, et al (2007) An ERF transcription factor in *Medicago truncatula* that is essential for Nod factor signal transduction. Plant Cell **19:** 1221–1234

Millenaar FF, van Zanten M, Cox MCH, Pierik R, Voesenek LACJ, Peeters AJM (2009) Differential petiole growth in *Arabidopsis thaliana*: photocontrol and hormonal regulation. New Phytol **184:** 141–152

Mitchum MG, Wang X, Davis EL (2008) Diverse and conserved roles of CLE peptides. Curr Opin Plant Biol **11:** 75–81

Miwa H, Kinoshita A, Fukuda H, Sawa S (2009) Plant meristems: *CLAVATA3/ESR*-related signaling in the shoot apical meristem and the root apical meristem. J Plant Res **122:** 31–39

Murray JD, Karas BJ, Sato S, Tabata S, Amyot L, Szczyglowski K (2007) A cytokinin perception mutant colonized by *Rhizobium* in the absence of nodule organogenesis. Science **315:** 101–104

Ni J, Clark SE (2006) Evidence for functional conservation, sufficiency, and proteolytic processing of the CLAVATA3 CLE domain. Plant Physiol **140:** 726–733

Nishimura R, Hayashi M, Wu G-J, Kouchi H, Imaizumi-Anraku H, Murakami Y, Kawasaki S, Akao S, Ohmori M, Nagasawa M, et al (2002) HAR1 mediates systemic regulation of symbiotic organ development. Nature **420:** 426–429

Nontachaiyapoom S, Scott PT, Men AE, Kinkema M, Schenk PM, Gresshoff PM (2007) Promoters of orthologous *Glycine max* and *Lotus japonicus* nodulation autoregulation genes interchangeably drive phloem-specific expression in transgenic plants. Mol Plant Microbe Interact **20:** 769–780

Nutman PS (1952) Studies on the physiology of nodule formation. III. Experiments on the excision of root-tips and nodules. Ann Bot (Lond) **16:** 79–101

Oelkers K, Goffard N, Weiller GF, Gresshoff PM, Mathesius U, Frickey T (2008) Bioinformatic analysis of the CLE signaling peptide family. BMC Plant Biol **8:** 1

Ogawa M, Shinohara H, Sakagami Y, Matsubayashi Y (2008) *Arabidopsis* CLV3 peptide directly binds CLV1 ectodomain. Science **319:** 294; erratum **Ogawa M, Shinohara H, Sakagami Y, Matsubayashi Y** (2008) Science **319:** 901

Ohyama K, Shinohara H, Ogawa-Ohnishi M, Matsubayashi Y (2009) A glycopeptide regulating stem cell fate in *Arabidopsis thaliana*. Nat Chem Biol **5:** 578–580

Okamoto S, Ohnishi E, Sato S, Takahashi H, Nakazono M, Tabata S, Kawaguchi M (2009) Nod factor/nitrate-induced *CLE* genes that drive HAR1-mediated systemic regulation of nodulation. Plant Cell Physiol **50:** 67–77

Oldroyd GED, Downie JA (2008) Coordinating nodule morphogenesis with rhizobial infection in legumes. Annu Rev Plant Biol **59:** 519–546

Oldroyd GED, Long SR (2003) Identification and characterization of *nodulation-signaling pathway 2*, a gene of *Medicago truncatula* involved in Nod factor signaling. Plant Physiol **131:** 1027–1032

Pacios-Bras C, Schlaman HRM, Boot K, Admiraal P, Langerak JM, Stougaard J, Spaink HP (2003) Auxin distribution in *Lotus japonicus* during root nodule development. Plant Mol Biol **52:** 1169–1180

Pierik R, Keuskamp DH, Sasidharan R, Djakovic-Petrovic T, de Wit M, Voesenek LACJ (2009) Light quality controls shoot elongation through regulation of multiple hormones. Plant Signal Behav **4:** 755–756

Quandt H-J, Pühler A, Broer I (1993) Transgenic root nodules of *Vicia hirsuta*: a fast and efficient system for the study of gene expression in indeterminate-type nodules. Mol Plant Microbe Interact **6:** 699–706

Radutoiu S, Madsen LH, Madsen EB, Felle HH, Umehara Y, Grønlund M, Sato S, Nakamura Y, Tabata S, Sandal N, et al (2003) Plant recognition of symbiotic bacteria requires two LysM receptor-like kinases. Nature **425:** 585–592

Radutoiu S, Madsen LH, Madsen EB, Jurkiewicz A, Fukai E, Quistgaard EMH, Albrektsen AS, James EK, Thirup S, Stougaard J (2007) LysM domains mediate lipochitin-oligosaccharide recognition and *Nfr* genes extends the symbiotic host range. EMBO J **26:** 3923–3935

Roche P, Debellé F, Maillet F, Lerouge P, Faucher C, Truchet G, Dénarié J, Promé J-C (1991) Molecular basis of symbiotic host specificity in *Rhizobium meliloti*: *nodH* and *nodPQ* genes encode the sulfation of lipo-oligosaccharide signals. Cell **67:** 1131–1143

Sambrook J, Fritsch EF, Maniatis T (1989) Molecular Cloning: A Laboratory Manual, Ed 2. Cold Spring Harbor Laboratory Press, Cold Spring Harbor, NY

Sato S, Nakamura Y, Kaneko T, Asamizu E, Kato T, Nakao M, Sasamoto S, Watanabe A, Ono A, Kawashima K, et al (2008) Genome structure of the legume, *Lotus japonicus*. DNA Res **15:** 227–239

Schauser L, Roussis A, Stiller J, Stougaard J (1999) A plant regulator controlling development of symbiotic root nodules. Nature **402:** 191–195

Schnabel E, Journet E-P, de Carvalho-Niebel F, Duc G, Frugoli J (2005) The *Medicago truncatula SUNN* gene encodes a *CLV1*-like leucine-rich repeat receptor kinase that regulates nodule number and root length. Plant Mol Biol **58:** 809–822

Searle IR, Men AE, Laniya TS, Buzas DM, Iturbe-Ormaetxe I, Carroll BJ, Gresshoff PM (2003) Long-distance signaling in nodulation directed by a CLAVATA1-like receptor kinase. Science **299:** 109–112

Sharma VK, Ramirez J, Fletcher JC (2003) The *Arabidopsis CLV3*-like (*CLE*) genes are expressed in diverse tissues and encode secreted proteins. Plant Mol Biol **51:** 415–425

Shiu S-H, Bleecker AB (2001) Receptor-like kinases from *Arabidopsis* form a monophyletic gene family related to animal receptor kinases. Proc Natl Acad Sci USA **98:** 10763–10768

Simon R, Stahl Y (2006) Plant cells CLEave their way to differentiation. Science **313:** 773–774

Smit G, de Koster CC, Schripsema J, Spaink HP, van Brussel AA, Kijne JW (1995) Uridine, a cell division factor in pea roots. Plant Mol Biol **29:** 869–873

Smit P, Raedts J, Portyanko V, Debellé F, Gough C, Bisseling T, Geurts R (2005) NSP1 of the GRAS protein family is essential for rhizobial Nod factor-induced transcription. Science **308:** 1789–1791

Stahl Y, Wink RH, Ingram GC, Simon R (2009) A signaling module controlling the stem cell niche in *Arabidopsis* root meristems. Curr Biol **19:** 909–914

Strabala TJ, O'Donnell PJ, Smit A-M, Ampomah-Dwamena C, Martin EJ, Netzler N, Nieuwenhuizen NJ, Quinn BD, Foote HCC, Hudson KR (2006) Gain-of-function phenotypes of many *CLAVATA3/ESR* genes, including four new family members, correlate with tandem variations in the conserved *CLAVATA3/ESR* domain. Plant Physiol **140:** 1331–1344

Takats ST (1990) Early autoregulation of symbiotic root nodulation in soybeans. Plant Physiol **94:** 865–869

Timmers ACJ, Auriac M-C, Truchet G (1999) Refined analysis of early symbiotic steps of the *Rhizobium-Medicago* interaction in relationship with microtubular cytoskeleton rearrangements. Development **126:** 3617–3628

Tirichine L, Sandal N, Madsen LH, Radutoiu S, Albrektsen AS, Sato S, Asamizu E, Tabata S, Stougaard J (2007) A gain-of-function mutation in a cytokinin receptor triggers spontaneous root nodule organogenesis. Science **315:** 104–107

van Brussel AAN, Bakhuizen R, van Spronsen PC, Spaink HP, Tak T, Lugtenberg BJJ, Kijne JW (1992) Induction of pre-infection thread structures in the leguminous host plant by mitogenic lipo-oligosaccharides of *Rhizobium*. Science **257:** 70–72

Van den Eede G, Deblaere R, Goethals K, Van Montagu M, Holsters M (1992) Broad host range and promoter selection vectors for bacteria that interact with plants. Mol Plant Microbe Interact **5:** 228–234

van Noorden GE, Ross JJ, Reid JB, Rolfe BG, Mathesius U (2006) Defective long-distance auxin transport regulation in the *Medicago truncatula super numeric nodules* mutant. Plant Physiol **140:** 1494–1506

van Spronsen PC, Grønlund M, Pacios Bras C, Spaink HP, Kijne JW (2001) Cell biological changes of outer cortical root cells in early determinate nodulation. Mol Plant Microbe Interact **14:** 839–847

Vervliet G, Holsters M, Teuchy H, Van Montagu M, Schell J (1975) Characterization of different plaque-forming and defective temperate phages in *Agrobacterium* strains. J Gen Virol **26:** 33–48

Wasson AP, Pellerone FI, Mathesius U (2006) Silencing the flavonoid

pathway in *Medicago truncatula* inhibits root nodule formation and prevents auxin transport regulation by rhizobia. Plant Cell **18:** 1617–1629

Whitford R, Fernandez A, De Groodt R, Ortega E, Hilson P (2008) Plant CLE peptides from two distinct functional classes synergistically induce division of vascular cells. Proc Natl Acad Sci USA **105:** 18625–18630

Wopereis J, Pajuelo E, Dazzo FB, Jiang Q, Gresshoff PM, de Bruijn FJ, Stougaard J, Szczyglowski K (2000) Short root mutant of *Lotus japonicus* with a dramatically altered symbiotic phenotype. Plant J **23:** 97–114

Yang W-C, de Blank C, Meskiene I, Hirt H, Bakker J, van Kammen A, Franssen H, Bisseling T (1994) *Rhizobium* Nod factors reactivate the cell cycle during infection and nodule primordium formation, but the cycle is only completed in primordium formation. Plant Cell **6:** 1415–1426